Oxidation mechanism of Si nanoparticles grown by plasma-CVD

K Nandi[1], S Chattopadhyay[2], S Ghosh[3], D Das[4] and D Jana[2]*

[1]Gurudas College, Kolkata-700 054, India
[2]Department of Physics, University of Calcutta, Kolkata-700 009, India
[3]St Xaviers' College, Kolkata-700 016, India
[4]Ramakrishna Mission Residential College, Narendrapur-700 103, 24-Parganas (N), W.B., India

E-mail · [4]d jana@cucc ernet in

Abstract · The oxidation behaviour and kinetics of oxidation of amorphous silicon nanoparticles grown by plasma-enhanced CVD were investigated. The hydrogen content of the particles has a great influence on the oxidation rate. Oxidation experiments performed in a thermo-balance in an atmosphere of dry air with a steady heating ramp show that the onset of oxidation shifts to higher temperatures when hydrogen contents were reduced by annealing in inert atmosphere. Apparently, the higher oxidation rate of as-grown particles is due to the large density of dangling bonds that are left behind just after the hydrogen is desorpted. The oxidation and dehydrogenation processes have been investigated by thermo-gravimetry (TG), differential scanning calorimetry (DSC), and X-ray diffraction (XRD) analysis The kinetics of oxidation of the completely dehydrogenated powders has been investigated under isothermal conditions. The kinetics was found to follow a parabolic law even at the relatively low temperature of oxidation indicating that the oxidation process is always controlled by oxygen diffusion. The structural changes and the growth of crystallites with oxidation temperature have also been studied.

Keywords : Oxidation kinetics, silicon nanoparticles, hydrogen, diffusion

PACS Nos. . 61.46.+w, 81.65.Mq, 82.20 Pm

1. Introduction

Study of the structural and optoelectronic properties of nano-sized amorphous silicon (a-Si) powders has been a subject of considerable interest to many researchers during the last ten years [1–6]. This is because Si based nanostructured materials were found to be very promising for their applications in the fabrication of the microeletronic devices. Nanoparticles and nanostructered materials exhibit quite different properties from their respective bulk materials and their properties are size dependent [7]. The growth of nanostructured thin films of silicon and its alloys has also been of considerable interest because of their possible application in a-Si based multijunction solar cells [8].

In contrast to crystalline Si, nanoparticles of Si has oxidation tendency at room temperature and it becomes quite significant at moderate temperatures. This higher oxidation rate at moderate temperatures may be attributed to the large amount of atomic hydrogen present in the particles with a high value of surface to volume ratio. This is a major drawback of the silicon based nanoparticles from their application point of view. Therefore, the oxidation kinetics of this material should be clearly

understood and the role of a large amount of atomic hydrogen present in it should be investigated.

In this paper, we report the oxidation behaviour of as-grown and dehydrogenated a-Si nanoparticles from the very early stage of oxidation in detail. The kinetics of oxidation are analyzed for the completely dehydrogenated particles. The advantage of working with nanoparticles is their very large specific surface area (>130 m²/gm) that allows us to monitor the oxidation process from very beginning through the related increase of mass recorded in TG. As it is shown in this report, kinetics of the process could be easily followed by measuring mass gain corresponding to the oxide layer thicknesses well below 1 nm. Our main objective was to investigate the role of hydrogen in the oxidation process. Previous works [5,9] have shown that the presence of hydrogen in this kind of nanoparticles makes them very sensitive to oxidation in air at moderate temperatures (the case of Si nanoparticles) or even at room temperature (SiC and SiCN nanoparticles).

2. Experimental

Silicon nanoparticles were grown at room temperature by plasma-enhanced chemical vapor deposition (PECVD) process from a

*Corresponding Author

silane precursor gas. Particles are known to nucleate from the free radicals formed during the plasma-ON period whereas they are deposited onto a solid substrate when the plasma is turned OFF. Their size is controlled by the residence time in the plasma. The transmission electron microscopy (TEM) images of the powder particles revealed that the particles are mostly spherical with mean diameter 20 nm and from electron diffraction patterns we came to know that they are amorphous. Another important structural characteristic feature is their high hydrogen content that comes from the precursor gas. By elementary analysis (EA), atomic hydrogen fraction of around 30% has been determined.

For XRD measurements, as-grown Si nanoparticles were oxidised at temperatures 200°C and 500°C for 1 hour in the libratherm (PID 300) furnace. In each case the annealing has been done in normal atmosphere and in furnace cooled condition. The structural modification after oxidation has been investigated by taking X-ray diffraction pattern of those samples in a PW 3710 diffractometer using Cu K_α radiation with a nickel filter. In each case, the scanning has been performed in the 2θ range 10^0 - 80^0 in a step size of 0.05^0.

Thermal treatments and oxidation experiments have been performed with a differential scanning calorimeter (DSC) DSC30 and a thermo-balance (TG) SDTA851 of METTLER. A high purity mixture of nitrogen (79%) and oxygen (21%) was used as the oxidation gas. Dehydrogenation experiments were performed by heat treatments in an inert atmosphere (nitrogen and argon) either with a steady heating ramp or under isothermal conditions for 1 hour. With DSC the heat evolved due to oxidation or dehydrogenation during steadily heating (at the rate of 10°C/min) of particles up to 600°C could be measured and thermograms were routinely corrected by the apparatus baseline. In case of thermogravimetric measurements, special care was taken on the isothermal experiments. To minimize the thermalization time of powders, we introduced the sample powder (kept in an alumina crucible) into the furnace of TG at the temperature of oxidation experiments, so that we could record the early stages of oxidation through the related increase of mass. All thermograms have also been corrected by the blank curve of the apparatus at the experimental conditions.

3. Results and discussion

Figure 1 shows the mass gain of the nanoparticles due to oxidation in synthetic air during heating with a steady ramp of 20°C/min for as-grown and partially or completely dehydrogenated powders. From the thermogram (curve a) a clearly defined onset of oxidation is observed at 280°C for as-grown particles. The slope of the curve indicates that the oxidation rate is enhanced just after this onset. The onset of oxidation is shifted progressively to higher temperatures with decrease in H-content of the powders.

The heat evolved during annealing of the as-grown powder with a steady heat ramp in argon atmosphere (dehydrogenation process) is shown in Figure 2. It is seen that the process of

dehydrogenation takes place in two steps, the main peak is at around 330°C. In order to evaluate the dynamics of the process
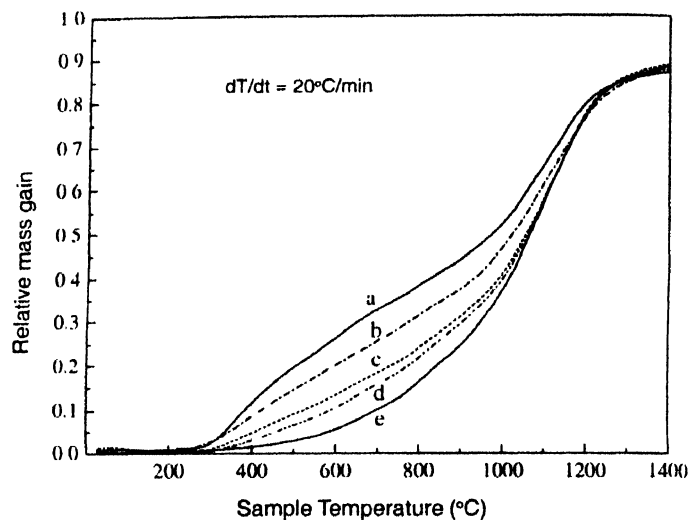

Figure 1. Mass gain of the nanoparticles due to oxidation in dry air during heating with a steady ramp (20°C/min) as grown (a), treated in inert atmosphere for 1 hr at 300°C (b), 350°C (c), 400°C (d), and 600°C (e). Curves b, c and d correspond to the partially dehydrogenated powders and curve (e) corresponds to the completely dehydrogenated powder
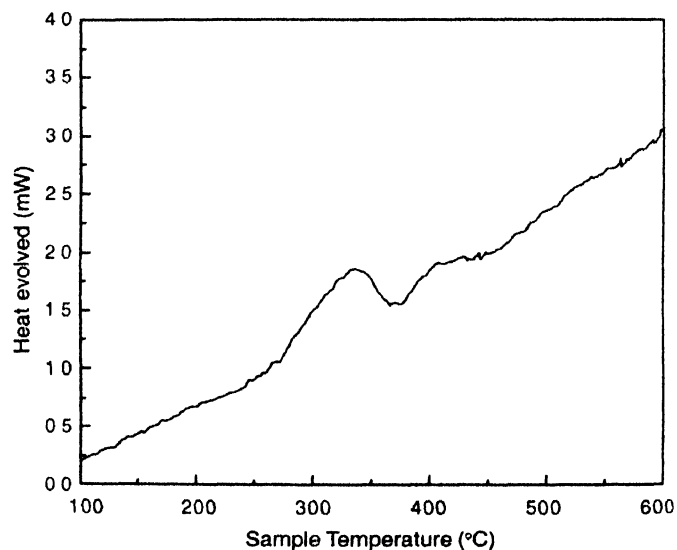

Figure 2. Heat evolved during annealing of the as-grown powder in nitrogen atmosphere

of mass loss due to the dehydrogenation in inert atmosphere, the rate of mass loss was fitted to a first order equation [10]

$$\frac{dm}{dt} = \left(\frac{kT}{h}\right)\left(m_{H_0} - m_H\right)\exp\left[(T\Delta S - \Delta H)/kT\right], \quad (1)$$

where dm/dt is the time derivative of mass change (%/s), ΔS is the activation entropy, ΔH is the enthalpy (=activation energy), m_{H_0}= mass of initial H-content (%) of the sample, m_{H} = % mass loss of sample at time 't', h = Planck's constant and k = Boltzmann constant, T = sample temperature. The fit of the experimental data is shown in Figure 3 and the activation energy

of the process is calculated. The calculated values of ΔH and ΔS are similar to the corresponding values for H-desorption from a-Si:H thin films [10]. Thus the process of H-desorption from a-Si nanopowder is basically same as that for a-Si:H thin films.
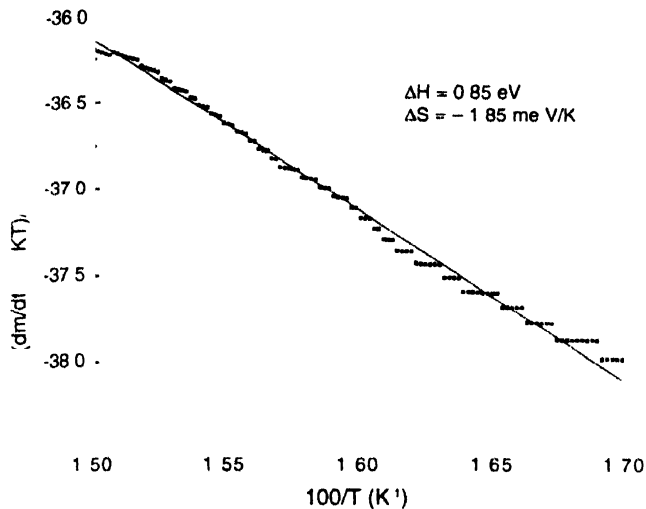

Figure 3. First order fit to the dehydrogenation process of as-grown a-Si nanopowder monitored by the related mass loss as recorded by TG

Figure 4 shows the curves of oxidation for completely dehydrogenated powder (produced by annealing the as-grown powder in nitrogen atmosphere at 600°C for 1h) performed under isothermal conditions in dry air at several temperatures. As expected, the mass gain increases monotonically with oxidation temperature. The curves of Figure 4 are fitted to a parabolic equation, $X^2 = Bt$, where 'X' is the relative mass gain in time 't' and B is the parabolic rate constant. From the temperature dependence of calculated B-values (Arhenius plot), the activation energy was found to be 0.85 eV.
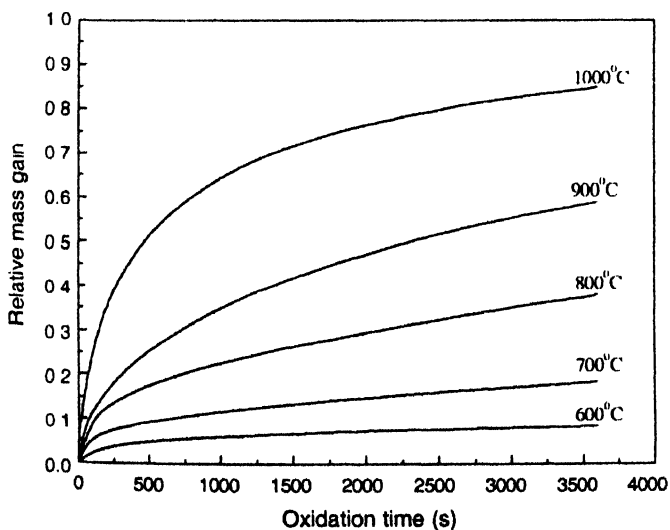

Figure 4. Oxidation isotherms performed in dry air at several temperatures for the completely dehydrogenated a-Si nanopowders.

From the XRD spectra (Figure 5) of the powder particles oxidised at 200°C and 500°C for 1 hour in dry air, development of

crystallites is evident from the signature of (111) orientation with peak position at ~28.50. The average crystallite sizes were
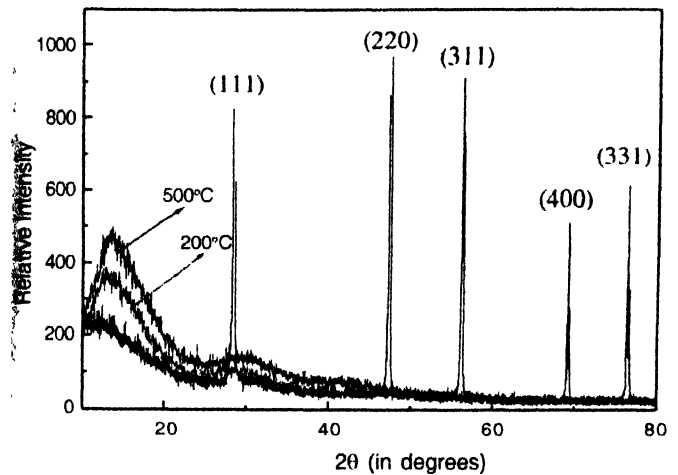

Figure 5. XRD spectra of a-Si nanoparticles oxidised in air at 200°C and 500°C for 1 hour For comparison, the XRD spectra of crystalline silicon is also shown

calculated from the broadened peaks of the X-ray diffractrogram using the Scherrer formula, $D = \dfrac{k\lambda}{\beta\cos\theta}$. The results so obtained are given in the following Table :

Sample oxidised at	Centre (deg)	Width (deg)	β (deg)	Average crystallite size (nm)
200°C	27 996	10 683	10 46524	1 68
500°C	28 979	8.0181	7.80034	2.26
Crystalline	28 429	0 21776		

Oxidation mechanism of as-grown powder is understood in view of its clearly defined onset temperature of oxidation, which is nearly the same as the temperature of H-evolution from a-Si nanoparticles and thin films. The shift of the oxidation onset to higher temperatures after partial dehydrogenation indicates that the presence of hydrogen is responsible for the high reaction rate of the as-grown particles. We can explain this fact in the following way. As a result of H-desorption, many of the dangling bonds created offer reactive site to oxygen. Once these are completely oxidised, the reaction rate would diminish. However, this concept of dangling bonds oxidation should be verified experimentally by *in situ* ESR measurements. The first stage of oxidation of as-grown particles would thus be reaction limited as no protective oxide layer is present. At higher temperatures, the oxidation is limited by the diffusion of oxygen through the silica formed in first stage as discussed in next section. The saturation trend of the curves of Figure 1 is due to the gradual reduction of surface area of particles as the oxidation proceeds and the oxidation approaches near completion at 1400°C for all of the samples.

Oxidation kinetics of crystalline silicon are generally described by using the linear-parabolic model of Deal and Grove

[11] in which the thickness of the oxide layer, X, grows according to the equation :

$$X^2 + AX = Bt \qquad (2)$$

where t is the oxidation time, B/A and B are the linear and parabolic rate constants, respectively. According to this model, the linear term takes into account the reaction of oxygen at the silicon-SiO_2 interface and the parabolic rate constant (B) is proportional to the diffusion coefficient of O_2 through the silica layer formed while oxidation proceeds. Although the existence of a linear term is well documented for crystalline Si-oxidation at lower temperatures[11,12], Doremus [13] observed that interface reaction is fast enough and thus is not a factor in the rate determining for the oxidation of Si. He proposed that a strain in the oxide film can result in linear-parabolic oxidation kinetics without a slow interface reaction. However, in another report [14], they observed that the linear-parabolic oxidation kinetics resulted from the diffusion of molecular oxygen through two different films, the main film of silicon dioxide and a thin interfacial film in which oxygen diffuses more slowly. A linear term results only when the film has a constant thickness. For nanoparticles, we observed parabolic oxidation kinetics even at relatively low temperatures of oxidation, indicating that the oxidation process is solely controlled by the diffusion of oxygen through the silica layer formed. For the dehydrogenated powder, the activation energy of parabolic rate constants we obtained (0.85 eV) is lower than that for the crystalline silicon (1.24 eV) [15]. Thus, for the nanoparticles, the oxide layer formed is less protective than the oxide layer formed on crystalline silicon.

4. Conclusion

The oxidation mechanism of amorphous silicon nanoparticles has been analyzed. A considerable influence of hydrogen content on the oxidation rate has been understood in view of the shift of the oxidation onset to higher temperatures when powders are partially dehydrogenated by annealing. At relatively high temperatures, oxidation is always controlled by diffusion of molecular oxygen through the oxide layer formed. When nano-

particles are oxidized, the oxide layer formed is less protective (as evident from the lower value of the activation energy), may be due to the formation of some kind of defects.

References

[1] G S Selwyn *Jpn. J Appl Phys* **32** 3068 (1993)

[2] J Dutta, I M Reaney, C Bossel, R Houriet and H Hofmann *Nanostructured Mater.* **6** 493 (1995)

[3] J Costa, G Sardin, J Campmany and E Bertran *Vacuum* **45** 1115 (1994)

[4] H Hofmeister, J Dutta and H Hofmann *Phys. Rev* **B54** 2856 (1996)

[5] J Costa, P Roura, J R Morante and E Bertran *J. Appl. Phys.* **83** 7879 (1998)

[6] R W Siegel *Nano Structured Materials* **4** 121 (1994)

[7] C Couerteil, J-L Dorier, J Dutta, Ch Hoolentein and A A Howling *J Appl. Phys.* **78** 61 (1995)

[8] P Rocai Cabarrocas *Mater Res. Soc. Symp. Proc.* **507** 855 (1998)

[9] G Viera, S N Sharma, J L Andújar, R Q Zhang J Costa and F Bertran *Vacuum* **52** 183 (1999)

[10] Yu L Khait, R Weil, R Beserman,W Beyer and H Wagner *Phys Rev.* **B42** 9000 (1990)

[11] B E Deal and A S Grove *J. Appl. Phys.* **36** 3770 (1965)

[12] L E Katz, VLSI Technology *Oxidation* (ed.) S M Sze (New York . McGraw Hill) (1983) p131

[13] R H Doremus *J. Appl Phys* **66** 4441 (1989)

[14] S C Kao and R H Doremus in *The Physics and Chemistry of SiO, and the Si-SiO₂ Interface*, (eds.) C RHelms and B E Deal (New York : Plenum Press) p 23 (1993)

[15] J A Costello and R E Tressler *J. Am. Ceram. Soc.* **69** 674 (1986)